

Electrophysiological Properties of Gap Junctions between Dissociated Pairs of Rat Hepatocytes

D. C. Spray,* R. D. Ginzberg,* E. A. Morales,* Z. Gatmaitan,‡ and I. M. Arias‡

*Department of Neuroscience, Albert Einstein College of Medicine, Bronx, New York 10461; and

‡Department of Physiology, Tufts University School of Medicine, Boston, Massachusetts 02111

Abstract. Physiological properties of isolated pairs of rat hepatocytes were examined within 5 h after dissociation. These cells become round when separated, but cell pairs still display membrane specializations. Most notably, canaliculi are often present at appositional membranes which are flanked by abundant gap and tight junctions. These cell pairs are strongly dye-coupled; Lucifer Yellow CH injected into one cell rapidly diffuses to the other. Pairs of hepatocytes are closely coupled electrically. Conductance of the junctional membrane is not voltage sensitive: voltage clamp studies demonstrate that g_j is constant in response to long (5 s) transjunctional voltage steps of either polarity (to $> \pm 40$ mV from rest). Junctional conductance (g_j) between hepatocyte pairs is reduced by exposure to octanol (0.1 mM) and by intracellular

acidification. Normal intracellular pH (pH_i), measured with a liquid ion exchange microelectrode, was generally 7.1–7.4, and superfusion with saline equilibrated with 100% CO_2 reduced pH_i to 6.0–6.5. In the pH_i range 7.5–6.6, g_j was constant. Below pH_i 6.6, g_j steeply decreased and at 6.1 coupling was undetectable. pH_i recovered when cells were rinsed with normal saline; in most cases g_j recovered in parallel so that g_j values were similar for pH_i obtained during acidification or recovery. The low apparent pK and very steep pH_i - g_j relation of the liver gap junction contrast with higher pK s and more gradually rising curves in other tissues. If H^+ ions act directly on the junctional molecules, the channels that are presumably homologous in different tissues must differ with respect to reactive sites or their environment.

LIVER is a tissue rich in gap junctions and it has therefore been a useful source of material for morphological, immunological, and biochemical studies of gap junction protein. The first detailed structural studies on gap junctional membranes included those in sections of intact liver stained with lanthanum (26), and the correlation of images of the gap junction in thin section with freeze-fracture replicas was aided by the abundance of this structure in liver (for review, see reference 2). Most recently, isolated hepatic gap junction membranes have provided material for high resolution structural studies using x-ray diffraction and low dose electron microscopy (18, 42, 47). The relatively large amount of junctional protein in liver has also allowed isolation for immunological and biochemical studies (for example, reference 11). Among exciting recent developments are antibodies that block junctional conductance (12, 43) and a partial sequence of amino acid residues comprising the major junctional protein (see reference 21) that has yielded a complete cDNA clone (23). Despite this progress, electrophysiological properties of hepatocyte gap junctions have remained poorly known, in part because of the small size of the cells and the opacity of the intact tissue (see references 9 and 24). Moreover, the component cells are complexly interconnected: coupled cells are arrayed in cords (6) so that models of current flow assuming three-dimensional uniformity cannot be used for spatial analysis (20).

The desirability of obtaining a dissociated hepatocyte preparation for many studies, in particular for experiments requiring homogeneity, has led to the development of procedures by which the tissue can be dissociated into single cells or small cell groups (see reference 3). In the past decade, various techniques have been refined so that the yield of healthy cells is high and their metabolic status is similar to that in normal liver (see reference 25); although presumably similar to those of the tissue *in vivo*, neither morphological nor physiological properties of surface membranes of cells shortly after they are dissociated have been described in detail.

In the present study we describe bile canaliculi and both gap and tight junctions between dissociated hepatocytes that by chance were isolated as pairs and characterize the cell pairs in terms of junctional communication. Gap junctional membranes between hepatocytes are insensitive to transjunctional or inside-outside voltage, but these cells are uncoupled by octanol exposure to and by intracellular acidification. Measurements with pH-sensitive microelectrodes show that the apparent pK is ~ 6.4 , lower than in other tissues. Around this pH value, however, the normal intracellular pH -junctional conductance (pH_i - g_j)¹ relation is remarkably steep (Hill coefficient ~ 8).

1. Abbreviations used in this paper: g_j , junctional conductance; pH_i , intracellular pH.

Preliminary accounts of some of these data have appeared (31, 34).

Materials and Methods

Cell Preparation

Cells were dissociated according to the procedure of Berry and Friend (3), using the perfusion medium of Leffert et al. (17). Briefly, rat liver was perfused with collagenase, minced, and incubated for 30 min. Cells were plated in RPMI 1640 (Gibco, Grand Island, NY) or in a hormonally defined medium (25; this medium consisted of RPMI 1640 [Gibco] supplemented with 100 U/ml penicillin, 100 meq/ml streptomycin, 50 ng/ml epidermal growth factor [Collaborative Research, Inc., Waltham, MA], 10 μ g/ml insulin, 10 μ g/ml glucagon, 5 μ g/ml linoleic acid/BSA [Miles Scientific, Naperville, IL], 20 mU/ml prolactin, 10 mU/ml growth hormone, 0.1 nM zinc, 0.1 μ M copper, and 0.3 nM selenium [trace elements from Johnson Matthey, Inc., Malvern, PA]) at a density of 5×10^5 cells/50-mm diam plastic petri dish (Falcon Labware, Becton, Dickinson & Co., Oxnard, CA). Hepatocytes were maintained in a 37°C, 5% CO₂ incubator and used within 5 h of plating for the studies reported here. Under these conditions hepatocytes survive for at least 1 wk in culture and after 24–48 h in culture can display nearly normal levels of tissue-specific mRNAs (25). Over the period of time considered here, no difference in electrophysiological properties of the cells (resting potential, input resistance, and g_j) were detected, in contrast to the changes that occur a few hours later (see reference 37). We therefore do not distinguish among these cells in this study, except to specify the latency from time of isolation to fixation for electron microscopy.

For studies with multiple microelectrodes the wall of the culture dish was cut with a heated nichrome wire at a height just above the fluid meniscus. Studies were generally conducted at 21°C after rinsing the cells with phosphate-buffered saline (PBS; Gibco) to which Hepes (5 mM, pH 7.4) was added.

Solutions

Electrophysiological experiments were generally performed on cell pairs continuously rinsed (0.5 ml/min in a 1-ml vol dish) with a simple saline solution (Dulbecco's PBS; Gibco) containing (in millimoles) NaCl (137), Na₂HPO₄ (8.1), KCl (2.7), KH₂PO₄ (1.5), CaCl₂ (0.9), MgCl₂ (0.50), to which was added 5 mM Hepes (pH 7.4). Solutions of octanol (0.2 mM) were freshly prepared in this medium. Lucifer Yellow CH (5% wt/vol) was prepared for injection in 150 mM LiCl and microelectrodes were backfilled with this solution. All chemicals were obtained from Sigma Chemical Co. (St. Louis, MO), unless otherwise noted.

Fluorescent Microscopy

Fluorescence micrographs of plated cells used for physiology were taken with xenon arc lamp illumination using a Nikon B filter block (excitation at 450–490 nm; emission above 520 nm) on a Nikon diaphot microscope (Nikon Inc., Instrument Div., Garden City, NY) using Plus-X film.

Electron Microscopy

Dissociated hepatocytes were fixed 1.5 h after plating with 2.5% ultrapure glutaraldehyde in 0.1 M cacodylate buffer at room temperature. Dishes of cells fixed at this time contained both attached cells and cells that had not yet settled. The medium was removed from the dishes and gently centrifuged in a 1-ml microcentrifuge tube to concentrate unattached cells. Supernatant medium was replaced with fixative and the cells gently resuspended and lightly pelleted again. Cells attached to the dish were fixed in situ after medium removal by flooding the dish with fixative. In both cases, after 30 min of fixation, specimens were rinsed thoroughly with cacodylate buffer. Cell pellets and the surrounding centrifuge tube were cut into slices (\sim 1-mm thick) for further processing; attached cells were postfixed and embedded in situ.

For thin section microscopy, pellet slices or dishes of cells were treated for 1 h with 1% OsO₄ in cacodylate buffer, washed, stained en bloc for 1 h with uranyl acetate, dehydrated, and embedded in Epon. For freeze fracture, the material was glycerinated (30% glycerine in cacodylate) to prevent ice crystal formation. Before freezing, pellets were removed from the surrounding tube, and attached cells were scraped from the culture dish with a coverslip. Specimens were then frozen sandwiched between flat gold disks in li-

quid nitrogen-cooled Freon 22 and transferred to a double replica device (Balzers, Hudson, NH). Fracturing was carried out using a Balzers model 301 freeze fracture machine equipped with an electron beam gun for platinum shadowing and a quartz crystal monitor for standardizing replica thickness. Specimens were fractured and replicated at -115°C ; replicas were cleaned overnight in bleach, rinsed in water several times, and examined with a Philips 300 electron microscope.

Electrophysiology

Cell pairs (which comprised a sizable fraction of the cultured cells) were either impaled with microelectrodes (20–30 M Ω , filled with 3 M KCl or KCltrate) connected to homemade electrometers with active bridge circuits or were penetrated with low resistance unpolished patch type electrodes (\sim 5–10 M Ω , filled with 150 mM KCl, 10 mM Hepes, 10 mM EGTA [pH 7.4]) connected to voltage clamps (see reference 45 for circuit diagrams and further procedural details). With bridge electrometers, electrode resistance was balanced before cell entry and was adjusted as necessary after penetration by neutralization of the fast initial resistive phase in the voltage trace in response to a 30-ms current pulse. For whole cell voltage clamp recordings, cells were slightly indented by the patch type electrode and gentle suction was applied to the rear of the electrode while monitoring in the voltage clamp mode the current produced by 1 mV, 30-ms pulses applied to the pipette. After a high resistance seal (\geq 1 G Ω) was formed, access to the cell interior was obtained with brief strong suction. Patch clamp circuits were then switched to the current clamp mode and series resistance was compensated using the criteria for bridge balance mentioned above. Finally, circuits were switched back to the voltage clamp mode for recording cell responses. Under current clamp conditions, current pulses were applied alternately to the two cells and conductances of junctional and nonjunctional membranes were calculated by applying the pi-tee transform to measured input and transfer resistances (32). Under whole cell voltage clamp, junctional current is passed by the clamp on one cell in response to a voltage command in the other; g_j is the junctional current divided by the transjunctional voltage (see reference 32).

pH-selective Microelectrodes

Microelectrodes were pulled from fiber-containing glass, and, if filled with 3 M KCl, would have had resistances of 20–30 M Ω . Tips were silanized by introducing 1 μ l 10% dichlorodimethylsilane (vol/vol in CCl₄) into the back of the electrode and then baking tip up in a vacuum oven at 200°C for 30 min. Ion exchange resin (neutral carrier proton exchanger from Fluka AG, Buchs, Switzerland) was then introduced into the electrode shank and the tip quickly filled. pH electrodes were backfilled with 150 mM potassium citrate buffered with citric acid to pH 6.5 and were calibrated before and after each experiment by measuring voltage response to immersion in buffered 150 mM KCl solutions in the range pH 6.0–7.5. Electrode response to a 1 pH-unit change was 90% of the final value within a few seconds; slope was between 55 and 58 mV/pH unit. pH_i was generally recorded differentially with respect to the voltage electrode in the same cell. Adequacy of intracellular placement of the ion selective electrode was established by comparison of steady-state responses of the voltage and ion selective electrodes in the same cell to a current pulse or voltage command (31). Reproducibility of pH_i measurements, judged from constancy of g_j -pH_i curves, was within 0.02–0.04 pH unit.

Results

General Appearance of Dissociated Cells

Soon after dissociation, hepatocytes lose the prismatic appearance that characterizes them in reconstructions from thick sections (6) and in scanning electron micrographs of the tissue (20); freshly dissociated cells are round and quickly adhere to the bottom of ordinary tissue culture dishes. In our preparation, cell pairs (Fig. 1 *a*) and small clusters were common; since cells were in most cases used soon after isolation, the cell pairs we studied were most likely ones in which gap junctions survived the dissociation procedure. Alternatively or in addition, some gap junctions may be newly formed.

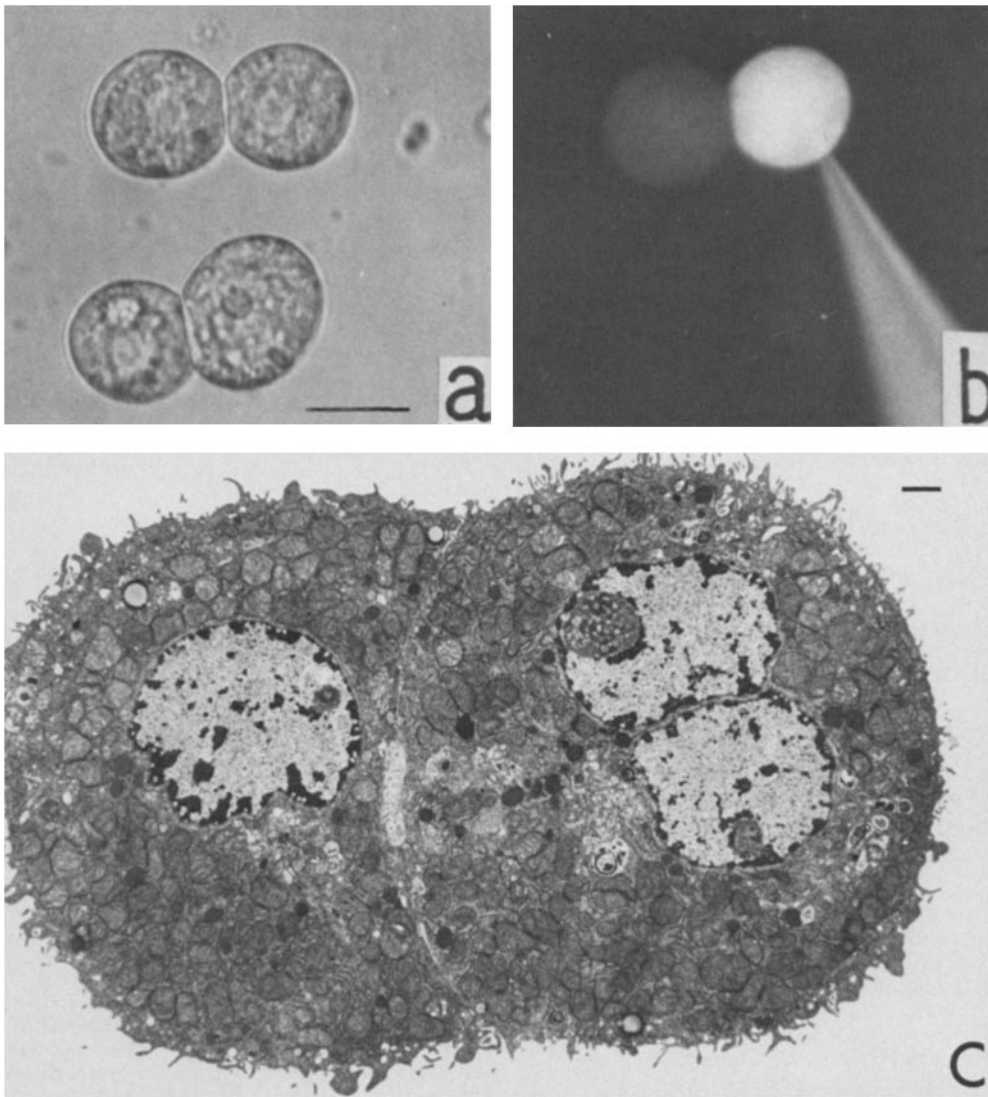


Figure 1. Light micrographs and ultrastructure of freshly dissociated hepatocyte pairs. Phase-contrast (a) and corresponding fluorescence (b) micrographs showing general appearance of dissociated rat hepatocytes. Soon after dissociation, pairs (a) of cells are present. The cells were dye-coupled; Lucifer Yellow spread from injected cells to their neighbors (b); note electrode placement. Bar (a and b), 20 μm . (c) Transmission electron micrograph of a dissociated pair of hepatocytes. One free surface (binucleate cell on right) contains many microvilli, reminiscent of hepatocyte surface bordering the space of Disse in vivo. The other free surface (cell on left) has cytoplasmic projections and fewer microvilli. Cytoplasm is dense, containing many organelles. The nuclei have sparse regions of dense chromatin, light nuclei, and prominent nucleoli. A bile canaliculus is maintained between the cells. Bar, 1 μm .

When Lucifer Yellow CH was injected into cells soon after dissociation (Fig. 1 b), the dye rapidly spread between or among coupled cells. Often dye spread nonhomogeneously when injected into one cell of a group (not illustrated). In some cases, nonuniform dye passage was attributable to the larger sink provided by the extra cell in that direction; in other cases, coupled cells filled at different rates, suggesting that not all cells were coupled equally well. Nevertheless, rapid dye transfer was always (hundreds of injections) observed between pairs of freshly dissociated cells (for example, in one series of experiments comparing rates of dye transfer at 21° and 37°C, there was no failure of dye transfer in 20 cell pairs in each of three dishes at either temperature).

Electron Microscopy

In material fixed shortly after dissociation (1.5 h), pairs or small groups (up to about six cells) of hepatocytes are frequently observed (Fig. 1 c). Cells of such pairs contain one, and occasionally more, prominent euchromatic nuclei. The cytoplasm is dense and filled with mitochondria and rough endoplasmic reticulum with occasional lipid vesicles. Some

of the free cell surface has numerous microvilli and presumably represents the area facing the space of Disse in vivo. The other free surface has cytoplasmic projections but fewer microvilli, and may have been appositional regions in vivo (note smooth area to the right of the right-hand cell in Fig. 1 c).

The appositional surfaces between freshly dissociated hepatocytes maintain most of the characteristics found in vivo, including intact bile canaliculi (upper central regions, Fig. 2, a and b). In both fractured (Fig. 2 a) and thin-sectioned (Fig. 2 b) specimens, microvillar projections into the canaliculi are flanked by tight junction networks (labeled *T* in Fig. 2 a, open arrow in Fig. 2 b). Small gap junctions are scattered within this network (arrowheads, Fig. 2 a); larger ones occur outside it (Fig. 2, c and d), merging with those beneath the tight junction network at the free surface. Where they are not filled with gap junctions, the interstices of tight junction networks are notably particle-poor. Gap junctions are less regularly surrounded by such particle-poor membrane (Fig. 2 c). Aside from variability in their size, the gap junctions are unremarkable. In P faces, gap junctions are composed of ~7-nm particles irregularly arranged in plaques (Fig. 2 c),

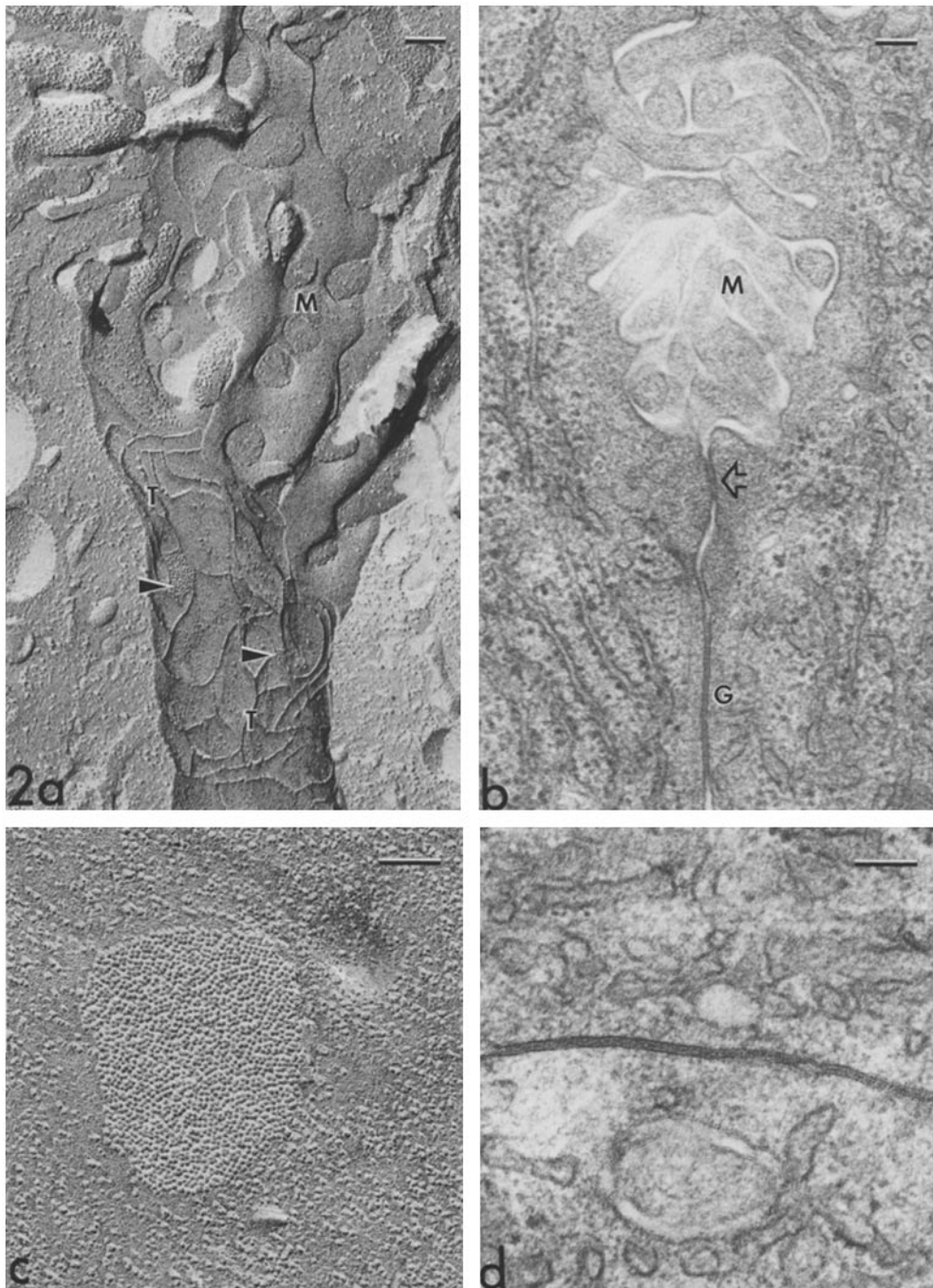


Figure 2. Ultrastructure of appositional areas. Freeze-fracture (a) and transmission (b) electron micrographs of equivalent canalicular and appositional regions between hepatocytes. Microvilli (M) extend into canalicular space. Tight junction ridges (T in a, arrow in b) and interspersed gap junction particle plaques (arrowheads) stand out in the P face of the appositional membrane in a, and a large gap junction (G) joins the appositional membranes of hepatocytes in b. Enlargements of hepatocyte gap junctions showing aggregated 7-nm P-face particles in fracture (c) and parallel unit membranes with 2–4-nm intercellular gap spanned by subunits in thin section (d). Bars, 0.1 μm .

and corresponding arrays of pits are found in E faces (not shown). The space or “gap” between membranes at thin-sectioned gap junctions is 2–4 nm and often is spanned by repeating densities (Fig. 2 d).

Electrophysiological Properties

Resting potentials of dissociated hepatocytes averaged ~ -40 mV (in one study using moderately high resistance [30 M Ω] electrodes, resting potentials averaged -39.8 ± 1.5 mV SD; $n = 38$), similar to values reported from liver cells in vivo (5, 9, 20). Injection of a current pulse into one cell of a pair showed that the cells are electrotonically coupled (Fig. 3 a),

also similar to the situation in vivo (4, 20, 24). The voltage in the injected cell appeared with a time constant ~ 10 –20 ms and a resulting voltage deflection in the second cell that was generally 20–60% or more of that observed in the first. Typically, input conductances measured with ordinary microelectrodes were in the range 20–50 nS and g_j was 0.1–1 μS (in one extensive series of experiments, g_j measured from cell pairs in sister cultures within 5 h of dissociation averaged 0.9 ± 0.1 μS SD; $n = 45$).

Junctional current is directly measured in dual voltage clamp experiments (Fig. 3 b) as the current that appears in one cell (I_2 in these records) in response to a voltage command in the other cell (see Materials and Methods). Voltage

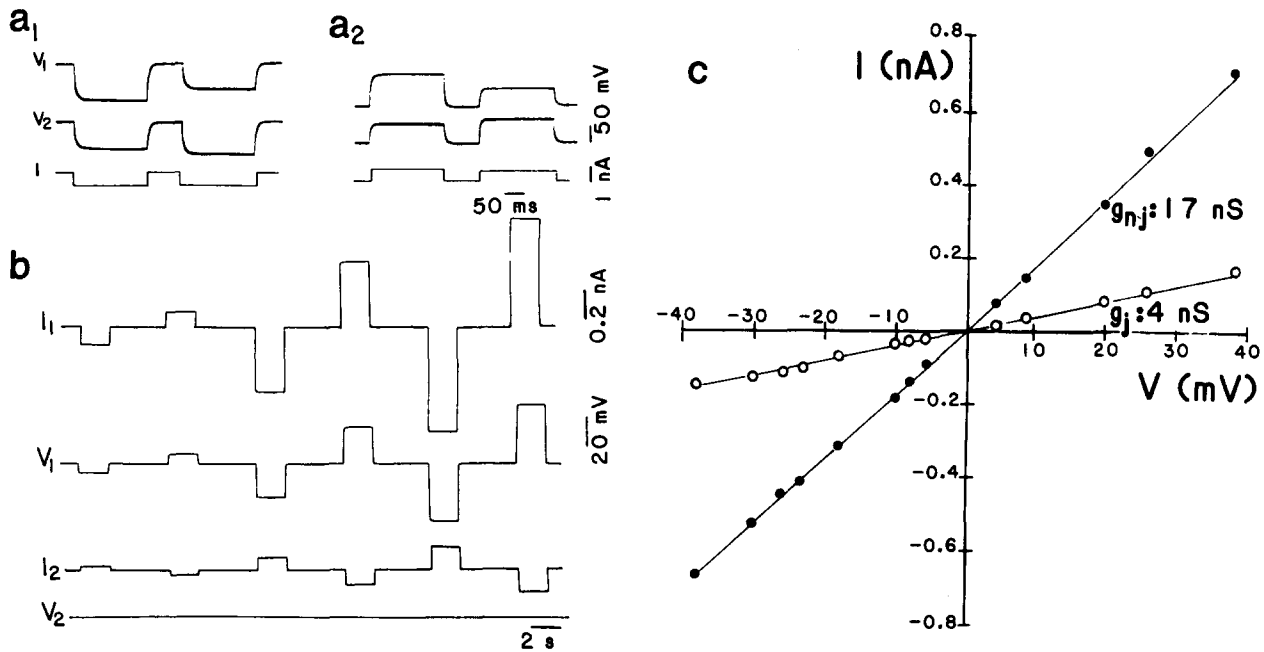


Figure 3. g_j between hepatocyte pairs is not voltage dependent. (a) Current (I), either hyperpolarizing (a_1) or depolarizing (a_2) passed in either cell produces voltage deflections in both cells (V_1 and V_2). (b) Under voltage clamp conditions, junctional current (I_2 , current in the cell whose voltage is constant) is proportional to negative or positive command voltages applied to cell 1 (V_1 ; input current seen in I_1) and does not change during the voltage step. This constancy indicates that g_j is not voltage dependent. (c) Current-voltage relationship for a pair of voltage clamped hepatocytes. The slopes, indicating conductances of junctional (O) and nonjunctional (●, only one non-junctional conductance is shown) membranes are linear, indicating lack of voltage dependence. Values for conductances (units: Siemens) appear alongside the slopes.

dependence of g_j was evaluated by passing long V_1 pulses of varying amplitudes (to 50 mV) and both polarities. During such voltage pulses (in more than 50 experiments on freshly dissociated hepatocytes from 12 rats), I_2 was constant and its magnitude was a linear function of V_1 (Fig. 3 b); g_j in hepatocytes is thus not appreciably affected by transjunctional voltage. There is also no dependence of g_j over the normal range of holding potentials (generally 0 to -40 mV) as is demonstrated in the current-voltage curves showing junctional and nonjunctional conductances for a pair of coupled cells (Fig. 3 c). The linearity of the current-voltage curve of the injected cell indicates that the nonjunctional membrane is not appreciably voltage dependent. Linearity of junctional and nonjunctional membranes is also suggested from *in vivo* studies (20), although the measurements are complicated by the geometry of the tissue.

Electrotonic coupling in several systems is reduced by extracellularly applied octanol (see references 15, 39 and 45). To determine whether this responsiveness is shared by hepatocyte gap junctions, 0.1 or 0.2 mM octanol dissolved in PBS was superfused over the cell pairs while coupling was measured (Fig. 4). Calculated g_j (plotted as connected dots, in the graph in Fig. 4) precipitously declined (by 80% over 15 s), while nonjunctional conductances (triangles) were not appreciably affected. Rinsing the preparation with PBS slowly restored g_j toward normal values (recovery to 75% within 3 min, Fig. 4; recovery to 95% within an additional 5 min, not shown here). The experiment illustrated here is typical of 24 responses of cell pairs from six dishes to superfusion with 0.1–0.2 mM octanol; in all cases g_j was abruptly reduced to <5% its initial value and in each case the effect was largely reversed by rinsing.

These data demonstrate that hepatocyte gap junctions are affected by a reagent that acts in other systems. Two other agents widely reported to affect g_j are cytoplasmic levels of H and Ca ions (see references 27, 33, 38, and 30 for review). To determine the extent to which g_j in hepatocytes is pH-dependent, g_j was measured in pairs of cells using either current injection (Fig. 5) or voltage clamp (Fig. 6), and pH_i was simultaneously monitored with a pH-sensitive microelectrode in one cell of the pair. Normal pH_i was 7.1–7.4 (mean 7.2 in 45 measurements) on cells in 18 dishes in Hepes-buffered medium (pH 7.4) but was generally considerably higher (7.8–8.1; measured in 18 cells in three cultures) in bicarbonate-buffered medium at ambient pCO_2 levels (extracellular pH, 8.2); this finding is consistent with others in intact tissue (5, 16).

To acidify the cells, medium equilibrated with 100% CO_2 was washed over the cells at various flow rates, allowing control of the rate and extent of acidification. In one experiment (Fig. 5) performed with current injection so that the coupling is directly observed, pH_i was reduced from 6.9 to 6.2 by exposure to CO_2 -equilibrated saline (between the arrows). Coupling between cells was markedly reduced; application of the pi-tee transform to input and transfer voltages showed that g_j was reduced by 95% while nonjunctional conductances were little affected (plot beneath graph). In the experiment shown in Fig. 6, performed under voltage clamp so that junctional current is directly observed and possible effects of potential are circumvented, the cell was initially at pH 7.8 in a bicarbonate-buffered medium. Exposure to 100% CO_2 at moderate flow rate reduced pH_i to ~ 6.9 with no change in g_j and very little effect on conductance of the nonjunctional membrane. Flow rate was then increased and the cell

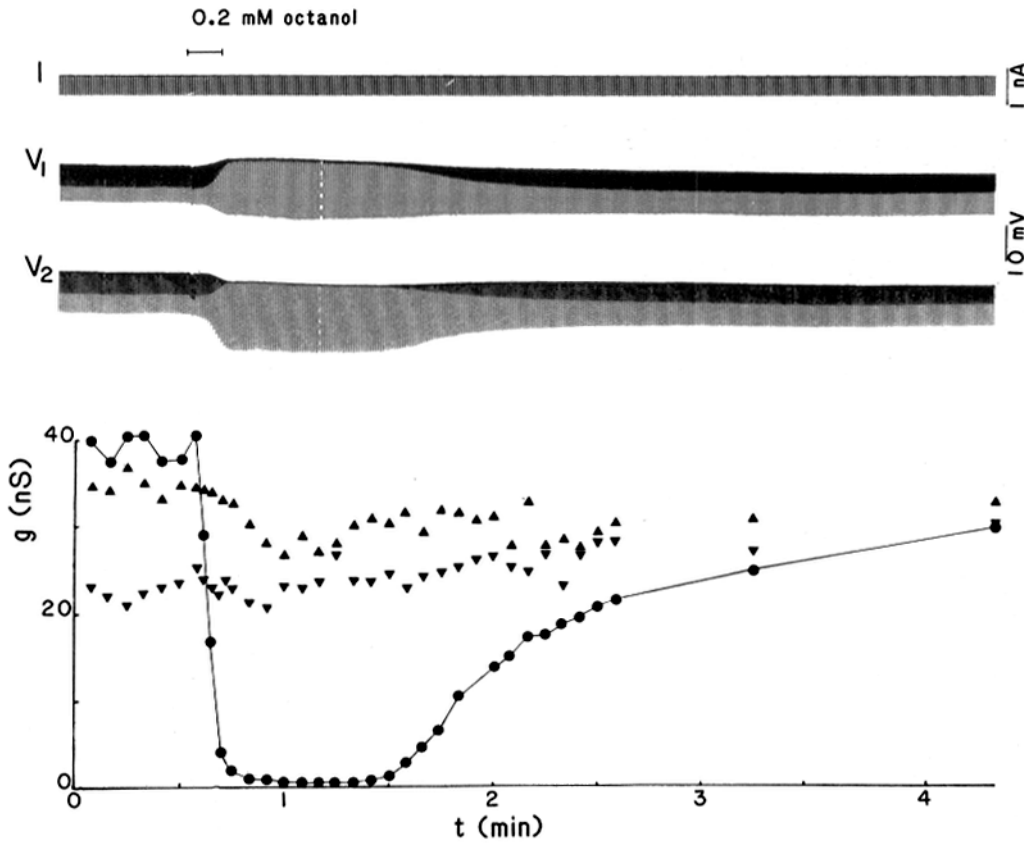


Figure 4. Reduction of coupling by octanol. (Top) Addition of 0.2 mM octanol to the medium (time of application indicated by bar at top of figure) reduced electrical coupling. Currents (I) are pairs of pulses applied alternately to cells 1 and 2. Edges of dark regions of the voltage responses (V_1 and V_2), transfer voltages associated with pulses in the other cell. Uncoupling in V_1 and V_2 , increase in input voltage and decrease in transfer voltage. (Bottom) Conductances of junctional (●) and nonjunctional membranes (▲, ▼) show that g_j is rapidly reduced by octanol and slowly recovers as the drug is washed away; nonjunctional conductances are not strongly affected.

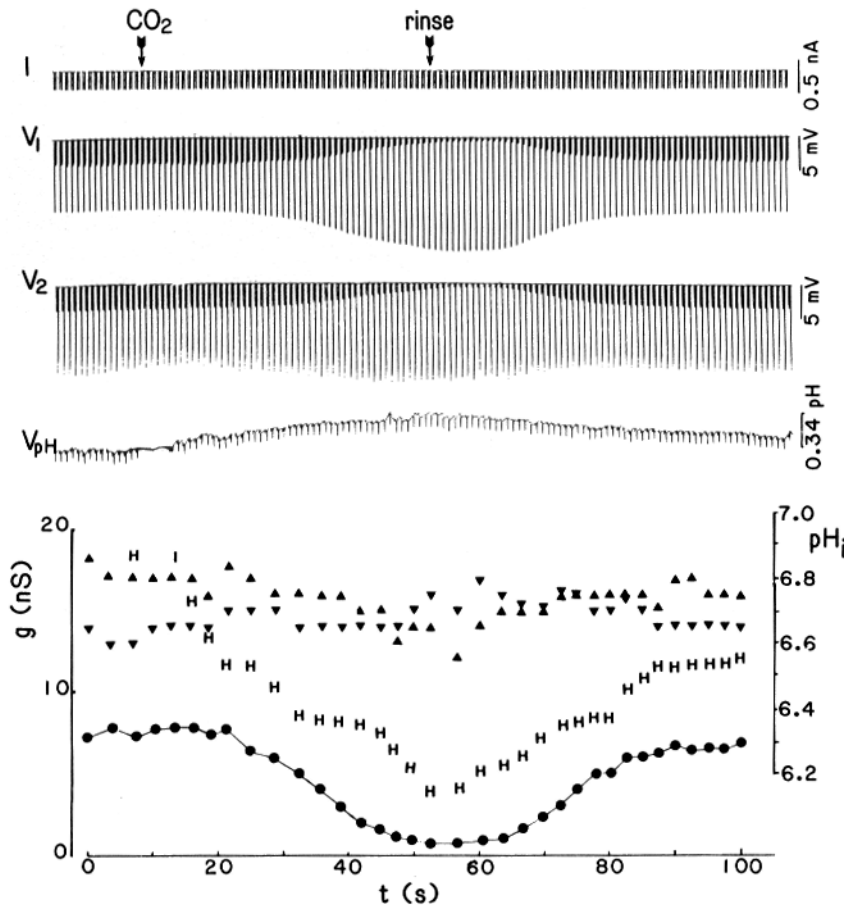


Figure 5. Uncoupling of hepatocytes by acidification: current clamp recording. Display as in Fig. 4 except voltage of pH electrode is also shown. Application of solution equilibrated with 100% CO₂ (between the arrows at the top of the figure) increased cytoplasmic acidity (V_{pH} , increased acidity upwards) and decreased electrical coupling (the transfer voltages in traces V_1 and V_2 decrease and the input voltages increase). Plot of junctional conductances (g_j , ●) and pH_i (H, scale on right) show that both decrease upon CO₂ exposure and recover on rinsing. Nonjunctional conductances (▲, ▼) are stable. The low pH_i at the beginning of this experiment is due to incomplete recovery from a prior acidification by CO₂.

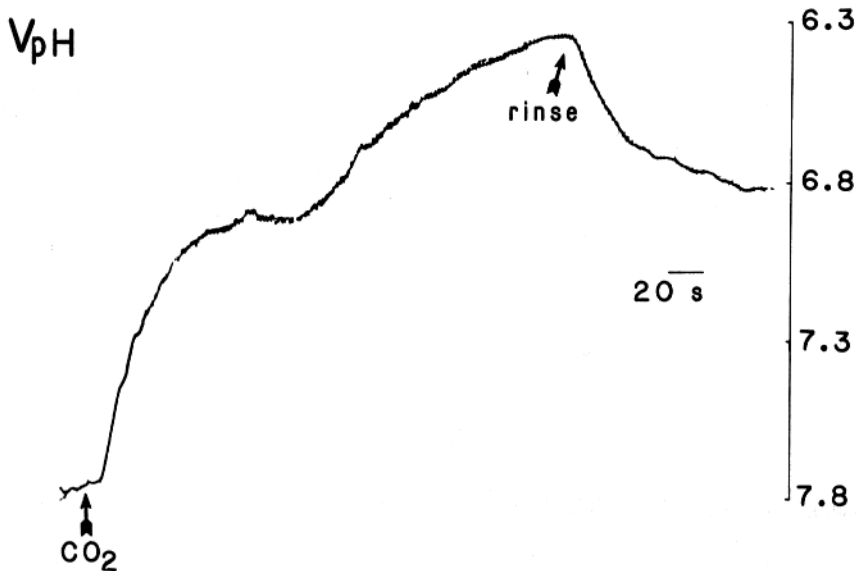
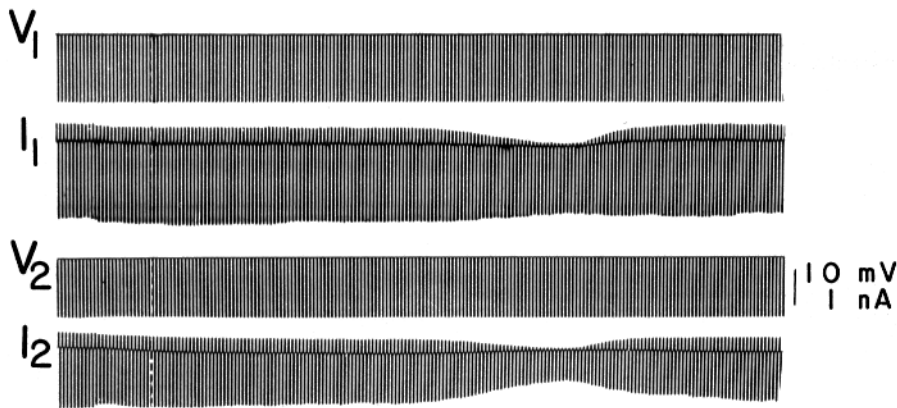


Figure 6. Effect of acidification on conductances of junctional and nonjunctional membranes: voltage clamp recording. pH_i is reduced (lowest trace) by exposure to CO_2 -equilibrated saline (between arrows). Hyperpolarizing voltage steps are alternately applied to the two cells. Junctional current (indicated by upward deflections above baseline in the current records I_1 and I_2) is unaffected by acidification to ~ 6.6 but is reduced by 90% between pH 6.6 and 6.3. Junctional currents recover upon rinsing. In these records the deflections downward from baseline are input currents that represent the sum of currents through junctional and nonjunctional membranes; changes in their amplitude with CO_2 exposure represent changes in g_j exclusively.

acidified further, reaching a final pH_i value of ~ 6.3 . Junctional currents were constant until pH_i reached ~ 6.5 and then decreased by $\sim 90\%$ between pH 6.5 and 6.3. The nonjunctional conductance of cell 2 also decreased over this pH range but there was little change in the nonjunctional membrane of cell 1. Decreasing the flow rate of the CO_2 -containing medium resulted in rapid recovery of pH_i to ~ 6.8 and recovery of g_j to control values. Rapidly flowing CO_2 reduced g_j by 90% in each of the more than 40 experiments on 16 cell pairs in which it was tested; g_j was largely restored in each case by rinsing in normal saline.

The relationship between g_j and pH_i during acidification and recovery was similar in eight experiments (each representing several acidification-recovery cycles) in which it was quantified (three of which are shown in Fig. 7). As was evident in the experimental data of Figs. 5 and 6, g_j is constant above pH 6.6 but between 6.6 and 6.3 it steeply declines so that for pH values more acidic than 6.2 no detectable g_j remains. These values of g_j at pH_i values obtained during acidification are fit by a form of the Hill equation (solid line) with an apparent pK of ~ 6.45 and a Hill coefficient (n) of ~ 8 (see Discussion). This value for n is the smallest that would satisfactorily encompass points on the upper and lower phases of the decline in g_j ; higher values (to 11) also

seem to adequately describe the pH_i - g_j relation for hepatocytes.

Measurements of g_j during acidification were generally the same for given pH_i values as seen during recovery (Figs. 5, 6, and 7). In two experiments, where pH_i changes were rapid and brief, the recovery of g_j became slower and in successive CO_2 exposures recovery of g_j lagged the recovery of pH_i .

Discussion

Morphological Comments

Pairs and groups of hepatocytes examined soon after the dissociation procedure maintain many of the differentiated structures characteristic of the adult liver. Presumably these cells have been only partly dissociated: some of the appositional surfaces are disrupted, as indicated by the presence of junctional remnants, while other surfaces maintain junctional contacts and specializations seen *in vivo* (20, 46). The identifiable microvillar free surfaces reminiscent of the intact hepatocyte lining the space of Disse, the correspondence of small microvilli-lined bile canaliculi, and the elaborate junctional network surrounding both support this interpretation

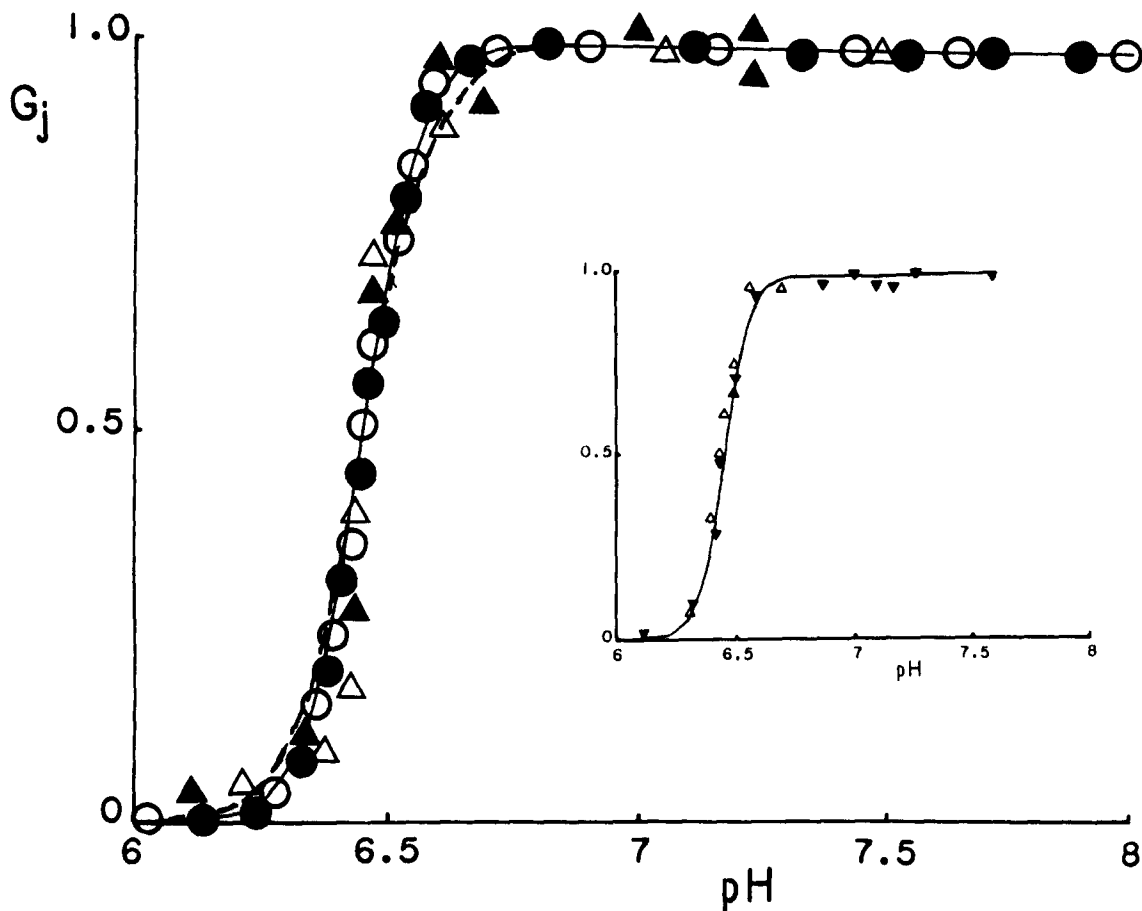


Figure 7. Correlation of g_j with pH_i . The relation between normalized junctional conductance (G_j) and decreasing pH_i in two voltage clamp experiments (O, ●) and two current clamp experiments (Δ , \blacktriangle); points are averages from several acidification-recovery cycles obtained by CO_2 exposure followed by rinsing with normal saline. The solid curve is a plot of the Hill equation ($G_j = K^n/(K^n + H^n)$) where G_j is normalized g_j , H is concentration of H^+ ions, K is the apparent dissociation constant, and n is the Hill coefficient. In this plot, fit by eye to the data, n is 8 and K corresponds to a pK of 6.45. The dashed curve is a plot of the Hill equation where $n = 6$ and K corresponds to an apparent pK of 6.38. Inset, G_j values during acidification (\blacktriangledown) and recovery (Δ).

and suggest that, at early times after dissociation, neither gap junction disappearance associated with regeneration (46) nor random re-association between hepatocytes (7) has yet occurred.

Comparative Considerations of Physiological Properties

The lack of voltage dependence of g_j in hepatocytes is similar to that found between a number of other vertebrate and invertebrate cell pairs (13, 39, other data reviewed in reference 30). Gap junctions in these tissues thus differ from those in which g_j is dependent on transjunctional voltage or the potential between the inside and outside the gap (22, 32, 34, 39, other data reviewed in reference 30).

Hepatocyte gap junctions are sensitive to extracellularly applied octanol, as are gap junctions between crayfish septate axons (15), pairs of cardiac myocytes (45), and squid, amphibian, and fish embryonic cells (39). The mechanism of this action is unclear, but is specific for octanol and heptanol (ethanol at 20 mM has no effect in any of these systems).

The resting pH_i reported here is consistent with that obtained by others applying nuclear magnetic resonance and

pH-sensitive microelectrodes to intact perfused liver (e.g., 5, 16). As was previously pointed out, high resting pH_i in the face of the very high pCO_2 of the portal circulation implies that buffer capacity of the cells must be enormous and that active H^+ extrusion could also play an important role in tissue homeostasis (5, 16). One candidate for such an extrusion mechanism is the Na/H antiport; indeed, these cells acidify profoundly when exposed to amiloride, which inhibits Na/H exchange (2).

The pH dependence of g_j in hepatocytes is markedly different from that in other tissues, where small changes in pH_i from the resting level may alter g_j (33; sensitivities of various gap junctions to pH are reviewed in reference 41). For liver, the pK is so low that pH gating is unlikely to be relevant to this gap junction under normal conditions. This low apparent pK possibly explains the previous report of lack of sensitivity of coupling within the intact liver exposed to CO_2 (19), a treatment likely to acidify cells to a lesser extent in the whole tissue than in culture.

In other tissues, a role for Ca ions has been suggested in control of junctional conductance, but in no case has the sensitivity of g_j to Ca been shown to be within a physiological range (27, 38, 40). Lack of sensitivity of hepatocyte gap junctions to Ca has recently been demonstrated in an elegant

study of the role of intracellular Ca and cytoplasmic contractile elements in the control of canalicular movement (44). In these experiments Ca injection sufficient to cause massive canalicular contractions did not block dye transfer through gap junctions located nearby. Our experimental results with Ca-selective microelectrodes indicate that Ca levels at least as high as 10 μ M (obtained with Ca ionophore and vasopressin application) do not reduce g_j (Spray, D. C., and J. C. Saez, unpublished observations) and are consistent with reported insensitivity in other systems.

Implications for Biochemical and Biophysical Studies

It seems reasonable that the pK and Hill coefficient contain information that is relevant for gap junction structure, since the closing of the channel at low pH presumably involves the binding of n or more protons to a site characterized by the apparent pK (33; while it seems likely to us that the binding site is an intrinsic portion of the channel molecule, we acknowledge that in most tissues action of a channel-associated modulatory molecule has not been excluded; see for example references 14 and 30 but see also 36).

The Hill coefficient may indicate the degree of cooperativity among subunits that comprise the channel. Presumably all gap junctions are dodecamers of subunits, hexamers being contributed by each cell. If there is one H⁺-binding site per subunit and occupation of all sites are required for channel closure, with maximum cooperativity n should be 12 (or 8 [the square of the Hill plot, see reference 33] if there are two independent hexamers in series, either of which can gate the channel). For liver, $n \cong 8$, consistent with a model where hexamers are arranged in series, conformational change of either hexamer causing channel closure. Alternatively, binding to 12 sites may be required for closure but with lower cooperativity (low cooperativity is apparently the case for other gap junctions regardless of closure mechanism, where values of n range from 1 to ~ 5 [see references 33, 45, and 41 for a review]).

Conductance of all gap junctions examined except lens is pH dependent although the slope and pK of the pH_i- g_j relations vary considerably from one tissue to another (see reference 41 for a review). In three tissues (lens, liver, and heart) partial sequences of the apparent junctional proteins are known. For lens there is no apparent homology with the other two, but for heart and liver there is 40% direct homology among residues comprising the n-terminal 25% of the molecule (21). Further evidence for homology is that an antibody prepared against alkali-extracted rat liver gap junctions crossreacts with 27,000-D proteins isolated from gap junctions obtained from a variety of tissues not including lens (11) and irreversibly blocks g_j and dye permeability when injected into pairs of rat ventricular myocytes, hepatocytes, and cultured sympathetic neurons (12). In lens, junctional conductance is apparently insensitive to acidification by CO₂ (29), whereas CO₂ and octanol rapidly and reversibly reduce g_j in heart cell pairs (45). Furthermore, conductance of cardiac gap junctions is insensitive to voltages over the range reported here; data on lens are unavailable. We conclude that the antigenically similar gap junction channels in heart and liver share responsiveness to certain stimuli and insensitivity to another.

The low apparent pK of the liver gap junction suggests that in this tissue, pH is of limited importance in regulating junc-

tional conductance. However, it also points out the value of this tissue for pharmacological experiments in which pH_i may vary; for example, in this tissue compounds such as cAMP can be delivered intracellularly as esterified derivatives without concern for effects on g_j of the minor accompanying acidification (28, 35).

Finally, this study provides functional criteria for identification of single channel currents measured in reconstituted systems as gap junctional of liver origin. Comparable macroscopic properties are unknown for lenticular gap junctions, although the lens is another rich source of material for reconstitution studies (8, 10). Hepatocyte gap junction channels ideally reconstituted would exhibit a lack of voltage dependence, blockade by moderate concentrations of octanol, strong pH dependence only in the range 6.6–6.2, lack of effect of low to moderate Ca concentrations, permeability to large ions, as well as blockade by certain gap junction antibodies. A recent report fulfills many of these expectations (36).

We are grateful to M. V. L. Bennett for critical comments on an earlier draft of this manuscript. Hepatocytes have been obtained from the Liver Research Center where G. Dudas and D. Withers prepared them. J. Zaviowitz constructed and calibrated many of the ion-selective microelectrodes used for these studies. We gratefully acknowledge his expert technical assistance. A New Initiative Award from National Institutes of Health (NIH) grant GM 30667 (to I. M. Arias) partially supported this work during its initial stages; the work has also been supported in part by NIH grants NS 16524, 07512, and 19830, and a McKnight Development Award (to D. C. Spray).

Received for publication 29 July 1985, and in revised form 24 March 1986.

References

1. Babayatsky, M., Z. Gatmaitan, D. C. Spray, and I. N. Arias. 1984. Sinusoidal amiloride-sensitive Na⁺/H⁺ antiport modulates pH_i and gap junction coupling in isolated paired rat hepatocytes. *Hepatology*. 4:1072. (Abstr.)
2. Bennett, M. V. L., and D. A. Goodenough. 1978. Gap junctions, electrotonic coupling and intercellular communication. *Neurosci. Res. Program Bull.* 16:373–486.
3. Berry, M. N., and D. S. Friend. 1969. High-yield preparation of isolated rat liver parenchymal cells. *J. Cell Biol.* 43:506–520.
4. Borek, C., S. Higashino, and W. R. Loewenstein. 1969. Intercellular communication and tissue growth. IV. Conductance of membrane junctions of normal and cancerous cells in culture. *J. Membr. Biol.* 1:274–293.
5. Cohen, R. D., R. M. Henderson, R. A. Iles, and J. A. Smith. 1982. Metabolic inter-relationships of intracellular pH measured by double-barrelled micro-electrodes in perfused rat liver. *J. Physiol. (Lond.)* 330:69–80.
6. Elias, H. 1953. Functional morphology of the liver. *Research in Service Med.* 37:1–26.
7. Feltkamp, C. A., and A. W. M. vander Waerden. 1983. Junction formation between cultured normal rat hepatocytes. *J. Cell Sci.* 63:271–286.
8. Girsch, S. J., and C. Perracchia. 1985. Lens cell-to-cell channel proteins. I. Self-assembly into lysosomes and permeability regulation by calmodulin. *J. Membr. Biol.* 83:217–225.
9. Graf, J., and O. H. Petersen. 1978. Cell membrane potential and resistance in liver. *J. Physiol. (Lond.)* 284:105–126.
10. Hall, J. E., and G. A. Zampighi. 1985. Protein from purified lens junctions induces channels in planar lipid bilayers. In *Gap Junctions*. M. V. L. Bennett and D. C. Spray, editors. Cold Spring Harbor Laboratory, Cold Spring Harbor, NY. 177–189.
11. Hertzberg, E., and R. V. Skibbens. 1984. A protein homologous to the 27,000 Dalton liver gap junction protein is present in a wide variety of species and tissues. *Cell*. 39:61–69.
12. Hertzberg, E. L., D. C. Spray, and M. V. L. Bennett. 1985. Antibodies to gap junctions block gap junctional conductance. *Proc. Natl. Acad. Sci. USA*. 82:2412–2416.
13. Johnston, M. F., and F. Ramon. 1982. Voltage independence of an electrotonic synapse. *Biophys. J.* 39:115–117.
14. Johnston, M. F., and F. Ramon. 1981. Electrotonic coupling in internally perfused crayfish segmented axons. *J. Physiol. (Lond.)* 317:509–518.
15. Johnston, M. V., S. A. Simon, and F. Ramon. 1980. Interaction of anesthetics with electrical synapses. *Nature (Lond.)* 286:498–500.
16. Kashiwagura, T., C. J. Deutsch, J. Taylor, M. Erecinska, and D. F. Wilson. 1984. Dependence of gluconeogenesis, urea synthesis, and energy metabolism of hepatocytes on intracellular pH. *J. Biol. Chem.* 259:237–243.

17. Leffert, N. L., K. S. Koch, and T. Moran. 1979. Liver cells. *Methods Enzymol.* 58:536-544.
18. Makowski, L. 1985. Structural domains in gap junctions: implications for the control of intercellular communication. In *Gap Junctions*. M. V. L. Bennett and D. C. Spray, editors. Cold Spring Harbor Laboratory, Cold Spring Harbor, NY. 5-12.
19. Meyer, D. J., and J.-P. Revel. 1981. CO₂ does not uncouple hepatocytes in rat liver. *Biophys. J.* 33:105a. (Abstr.)
20. Meyer, D. J., S. B. Yancey, and J.-P. Revel. 1981. Intercellular communication in normal and regenerating rat liver: a quantitative analysis. *J. Cell Biol.* 91:505-523.
21. Nicholson, B. J., L. J. Takemoto, M. W. Hunkapillar, L. E. Hood, and J.-P. Revel. 1983. Differences between the liver gap junction protein and lens MIP26 from rat: implications for tissue specificity of gap junctions. *Cell.* 32:967-978.
22. Obaid, A. L., S. J. Socolar, and B. Rose. 1983. Cell-to-cell channels with two independently regulated gates in series: analysis of junctional conductance modulation by membrane potential, calcium and pH. *J. Membr. Biol.* 73:69-89.
23. Paul, D. 1986. Molecular cloning of cDNA for rat liver gap junction protein. *J. Cell Biol.* 103:123-134.
24. Penn, R. D. 1966. Ionic communication between liver cells. *J. Cell Biol.* 29:171-174.
25. Reid, L. M., and D. M. Jefferson. 1984. Cell culture studies using extracts of extracellular matrix to study growth and differentiation in mammalian cells. In *Mammalian Cell Culture*. J. P. Mather, editor. Plenum Publishing Corp., New York. 239-280.
26. Revel, J.-P., and M. J. Karnovsky. 1967. Hexagonal arrays of subunits in intercellular junctions of the mouse heart and liver. *J. Cell Biol.* 33:C7-C12.
27. Rose, B., and W. R. Loewenstein. 1975. Permeability of cell junctions depends on local cytoplasmic calcium activity. *Nature (Lond.)*. 254:250-252.
28. Saez, J. C., D. C. Spray, E. L. Hertzberg, A. C. Nairn, P. Greengard, and M. V. L. Bennett. 1986. cAMP increases junctional conductance and stimulates phosphorylation of the 27 kDa principal gap junction polypeptide. *Proc. Natl. Acad. Sci. USA.* 83:2473-2477.
29. Schuetze, S. M., and D. A. Goodenough. 1982. Dye transfer between cells of the embryonic chick lens becomes less sensitive to CO₂ treatment with development. *J. Cell Biol.* 92:694-705.
30. Spray, D. C., and M. V. L. Bennett. 1985. Physiology and pharmacology of gap junctions. *Annu. Rev. Physiol.* 47:281-303.
31. Spray, D. C., R. D. Ginzberg, E. A. Morales, M. V. L. Bennett, M. Babayatsky, Z. Gatmaitan, and I. M. Arias. 1984. Physiological and morphological properties of gap junctions between dissociated pairs of rat hepatocytes. *J. Cell Biol.* 99(4, Pt. 2):344a. (Abstr.)
32. Spray, D. C., A. L. Harris, and M. V. L. Bennett. 1981. Equilibrium properties of a voltage dependent junctional conductance. *J. Gen. Physiol.* 77:75-94.
33. Spray, D. C., A. L. Harris, and M. V. L. Bennett. 1981. Gap junctional conductance is a simple and sensitive function of intracellular pH. *Science (Wash. DC)*. 211:712-715.
34. Spray, D. C., and E. L. Hertzberg. 1985. Biophysical properties of gap junction channels. *Biophys. J.* 47:505a. (Abstr.)
35. Spray, D. C., J. Nerbonne, A. C. Campos de Carvalho, A. L. Harris, and M. V. L. Bennett. 1984. Substituted benzyl acetates: a new class of compounds that reduce gap junctional conductance by cytoplasmic acidification. *J. Cell Biol.* 99:174-179.
36. Spray, D. C., J. C. Saez, D. Brosius, M. V. L. Bennett, and E. L. Hertzberg. 1986. Isolated liver gap junctions inserted into bilayers: gating of transjunctional currents is similar to that in isolated pairs of rat hepatocytes. *Natl. Acad. Sci. USA.* In press.
37. Spray, D. C., J. C. Saez, W. A. Gregory, and E. L. Hertzberg. 1985. Gap junctions between cultured hepatocytes are maintained by cAMP derivatives, agents that disrupt or stabilize the cytoskeleton, and reduced intracellular pH. *J. Cell Biol.* 101(5, Pt. 2):178a. (Abstr.)
38. Spray, D. C., J. H. Stern, A. L. Harris, and M. V. L. Bennett. 1982. Comparison of sensitivities of gap junctional conductance to H⁺ Ca ions. *Proc. Natl. Acad. Sci. USA.* 79:441-445.
39. Spray, D. C., R. L. White, A. Campos de Carvalho, A. L. Harris, and M. V. L. Bennett. 1984. Gating of gap junction channels. *Biophys. J.* 45:219-230.
40. Spray, D. C., R. L. White, F. Mazet, and M. V. L. Bennett. 1985. Control of gap junction conductance. *Am. J. Physiol.* 248:H753-764.
41. Spray, D. C., R. L. White, V. Verselis, and M. V. L. Bennett. 1985. General and comparative physiology of gap junction channels. In *Gap Junctions*. M. V. L. Bennett and D. C. Spray, editors. Cold Spring Harbor Laboratory, Cold Spring Harbor, NY. 355-366.
42. Unwin, N. T., and G. Zampighi. 1980. Structure of the junction between communicating cells. *Nature (Lond.)*. 283:545-549.
43. Warner, A. E., S. Guthrie, and N. B. Gilula. 1984. Antibodies to gap junctional protein selectively disrupt junctional communication in early amphibian embryos. *Nature (Lond.)*. 311:127-131.
44. Watanabe, S., and M. J. Phillips. 1984. Ca²⁺ causes active contraction of bile canaliculi: direct evidence from microinjection studies. *Proc. Natl. Acad. Sci. USA.* 81:6164-6168.
45. White, R. L., D. C. Spray, A. C. Campos de Carvalho, B. A. Wittenberg, and M. V. L. Bennett. 1985. Some physiological and pharmacological properties of cardiac myocytes dissociated from adult rat. *Am. J. Physiol.* 249:c447-c455.
46. Yee, A. G., and J. P. Revel. 1978. Loss and reappearance of gap junctions in regenerating liver. *J. Cell Biol.* 78:554-564.
47. Zampighi, G., and S. A. Simon. 1985. The structure of gap junctions as revealed by electron microscopy. In *Gap Junctions*. M. V. L. Bennett and D. C. Spray, editors. Cold Spring Harbor Laboratory, Cold Spring Harbor, NY. 13-22.